CrossMark

Sound speed estimation and source localization with linearization and particle filtering

Tao Lin and Zoi-Heleni Michalopoulou[a)]
Department of Mathematical Sciences, New Jersey Institute of Technology, Newark, New Jersey 07102

(Received 6 August 2013; revised 2 December 2013; accepted 28 January 2014)

A method is developed for the estimation of source location and sound speed in the water column relying on linearization. The Jacobian matrix, necessary for the proposed linearization approach, includes derivatives with respect to empirical orthogonal function coefficients instead of sound speed directly. First, the inversion technique is tested on synthetic arrival times, using Gaussian distributions for the errors in the considered arrival times. The approach is efficient, requiring a few iterations, and produces accurate results. Probability densities of the estimates are calculated for different levels of noise in the arrival times. Subsequently, particle filtering is employed for the estimation of arrival times from signals recorded during the Shallow Water 06 experiment. It has been shown in the past that particle filtering can be employed for the successful estimation of multipath arrival times from short-range data and, consequently, in geometry, bathymetry, and sound speed inversion. Here probability density functions of arrival times computed via particle filtering are propagated backward through the proposed inversion process. Inversion estimates are consistent with values reported in the literature for the same quantities. Last it is shown that results are consistent with estimates resulting from fast simulated annealing applied to the same data.
© *2014 Acoustical Society of America*. [http://dx.doi.org/10.1121/1.4864787]

PACS number(s): 43.30.Pc, 43.60.Uv, 43.30.Wi [SED] Pages: 1115–1126

I. INTRODUCTION

Estimating the location of an underwater sound source is an important practical problem with well known and long standing applications in defense. More recently applications in environmental studies have been made imperative and are of serious concern. Beyond source location there is a rich set of environmental information available in the traditional data source. The time-series data recorded at arrays of hydrophones contain information on properties of the ocean through which the sound has traveled. Extracting this information from the noise contaminated data is a broader objective of active defense and environmental sciences research programs. Inverse theory is a critical modeling component of those programs, central to both estimation goals. Open problems are considerable with computational efficiency being of particular concern. We propose a novel linearization procedure that directly addresses the computational burden while retaining estimation fidelity.

A popular approach for inversion is matched-field processing (MFP).[1] This requires a combination of wave propagation modeling for the generation of replica fields at receiving phones and a decision rule that estimates model parameters entering the replica calculation. Inversion is performed by identifying those values of the model parameters that maximize a similarity measure between replica and true acoustic fields. Although MFP was originally used for source localization, it was subsequently applied to estimation of environmental parameters as well.[2–8] MFP, when applied for the estimation of environmental parameters, is often referred to as matched-field inversion (MFI).

MFP/MFI has been applied with excellent results both to synthetic and real data. However, as a full-field matching approach, this method requires that the full acoustic field is calculated at a set of receiving phones and compared through the selected measure of similarity to the received acoustic data. Many parameters affect sound propagation and, thus, enter the replica field calculation and estimation process. As a result, although we may only be interested in estimating the source location and a limited set of environment-related parameters, more factors need to be considered. Such factors are the properties of the bottom sediment because those affect the full field: Uncertainty regarding these parameters has to be incorporated in the estimation process for accurate inversion. Therefore the computational load of MFI methods can be substantial, especially when the number of unknown or uncertain parameters is large and the signal carries broadband information. Global optimization techniques have been successfully developed and applied for the acceleration of matched field methods,[5–7,9,10] but, even with such approaches, the issue of expensive computations remains.

As an alternative, to avoid multiple replica field calculation, many attempts have been made to investigate the potential for matching only select features of the acoustic field to corresponding replica features. Knowledge of arrival times of distinct paths that the sound follows from source to receivers rather than the full field can facilitate both source localization and ocean property estimation. Different inversion methods have been implemented in this direction.[11–16] Also fast linearization schemes have been successfully implemented in several aspects of inversion in underwater acoustics and seismic studies.[14–19]

[a)]Author to whom correspondence should be addressed. Electronic mail: michalop@njit.edu

Redistribution subject to ASA license or copyright; see http://acousticalsociety.org/content/terms. Download to IP: 128.235.24.147 On: Sun, 23 Mar 2014 17:27:53

In this paper, a linearization inversion method is developed that employs select ray paths [direct (D), first surface reflection (SR), and first bottom reflection (BR)] for source localization and estimation of bottom depth and sound speed profile. Previously, such methods have been employed for the estimation of bias in sound speed[14] or for isovelocity profile estimation but not for complete sound velocity profile estimation in general situations. In our case, the linearization process inverts for complete profiles, bypassing the difficult incorporation of such profiles in the Jacobian matrix by calculating derivatives with respect to empirical orthogonal function (EOF) coefficients.[20]

Before applying the linearization estimation method, it is important to have accurate multipath arrival times that will be used as input to the inversion process. A particle filtering method for the estimation of such arrivals was presented in Ref. 21 and was demonstrated to provide more reliable results than conventional approaches. In the same reference, successful localization with real data was demonstrated using arrival times and corresponding probability density functions (PDFs) extracted via particle filtering.

The new method is first tested on synthetically generated arrival times by assuming that the extracted times follow a Gaussian distribution. The approach is then applied to arrival times extracted via particle filtering on Shallow Water 06 (SW06) data. Inversion for source location, array tilt, water column depth, and EOF coefficients with SW06 data and global optimization methods has been discussed in Refs. 22 and 23. Results presented in those references are used here for comparison.

The paper is organized as follows: Sec. II discusses the linearization scheme introduced in this paper. Emphasis is placed on sound speed inversion with EOFs. Section III presents results by applying the proposed method to synthetic data. Section IV discusses the SW06 data and the particle filter that extracts distinct path arrival times and also presents inversion results from the SW06 time series. Simulated annealing results are also presented for comparison. Conclusions follow in Sec. V.

II. INVERSION WITH LINEARIZATION

A. The linear system

Equation (1) in the following text reflects the fact that the arrival time t of each path is a function of the source location (range r and source depth z_s), water column depth WD, sound speed $c(z)$, and transmission instant t_0 for the underwater problem of interest,[14,16]

$$t = \tau(\tau, z_s, WD, c(z)) + t_0, \tag{1}$$

where τ represents the ray travel time.

Generalizing, we can write

$$\mathbf{t} = \mathbf{f}(\mathbf{q}), \tag{2}$$

where $\mathbf{t}$ is the vector of measured/estimated travel times; $\mathbf{f}$ represents the forward or acoustic model that relates the measurements to a set of parameters; $\mathbf{q}$ represents the vector containing the parameters to be estimated,

$$\mathbf{q} = [\mathrm{r}, z_s, WD, c(z), t_0]. \tag{3}$$

Other parameters such as sound speed and thickness of sediments enter Eq. (1) when rays that have interacted with the sediments are considered.

For our problem, the signal is received at N hydrophones of a vertical line array (VLA). If three characteristic ray paths (D, SR, and BR, here) are employed, that is, $K=3$, where K is the number of paths, there will be a total of $KN=3N$ arrival time measurements, which serve as our data.

For our acoustic inverse problem, vector $\mathbf{q}$ is estimated using the measured travel times and forward model $\mathbf{f}$, relying on ray theory. Because of the nature of our data (time) and its relationship to the geometry of the problem and also water column sound speed, the inverse process in our case is quasi-linear: Linearizing the problem locally has been shown to lead to accurate solutions in an efficient manner.[14,16]

A linear approximation to Eq. (2) can be obtained as[14,16,18,19]

$$\mathbf{t} = \mathbf{f}(\mathbf{q_0}) + \mathbf{J}\delta\mathbf{q}, \tag{4}$$

where $\mathbf{q_0}$ is a vector of initial conditions for $\mathbf{q}$, $\delta\mathbf{q}$ is the model perturbation that provides a "correction" to the initial model parameters as will be explained in the following text, and $\mathbf{J}$ is the Jacobian matrix that contains the partial derivatives of time with respect to the unknown parameters for each path. That is,

$$J = \begin{pmatrix} \frac{\partial t_1}{\partial q_1} & \frac{\partial t_1}{\partial q_2} & \cdots & \frac{\partial t_1}{\partial q_M} \\ \frac{\partial t_2}{\partial q_1} & \frac{\partial t_2}{\partial q_2} & \cdots & \frac{\partial t_2}{\partial q_M} \\ \cdots & \cdots & \cdots & \cdots \\ \frac{\partial t_{\mathrm{KN}}}{\partial q_1} & \frac{\partial t_{\mathrm{KN}}}{\partial q_2} & \cdots & \frac{\partial t_{\mathrm{KN}}}{\partial q_M} \end{pmatrix}. \tag{5}$$

Vector $\mathbf{q}$ consists of M variables.

By introducing $\delta\mathbf{t} = \mathbf{t} - \mathbf{f}(\mathbf{q_0})$, Eq. (4) leads to

$$\mathbf{J}\delta\mathbf{q} = \delta\mathbf{t}. \tag{6}$$

Equation (6) reflects a linear relationship between arrival time differences and perturbations of parameters $\mathbf{q}$.

More specifically, quantities $\delta\mathbf{t}$ of Eq. (6) represent the differences between path arrivals in the real signals and synthetic arrivals generated for a set of initial values for the unknown parameters. Through Eq. (6), corrections $\delta\mathbf{q}$ for the unknown parameters are obtained that provide a better match between real and replica times. The system needs to be solved iteratively until it converges. At every step, the results from the previous iteration are employed as the new initial conditions.

Equation (6) generally leads to an overdetermined linear system (for our data we consider $N=14$ hydrophones and $K=3$ arrival times for each phone; we are inverting for seven parameters—source range and depth, water depth, three EOF coefficients, and time instant for synthetic data

Redistribution subject to ASA license or copyright; see http://acousticalsociety.org/content/terms. Download to IP: 128.235.24.147 On: Sun, 23 Mar 2014 17:27:53

and we also include tilt for the real data inversion). Least squares can be used for the solution of the system; more details will follow in Sec. II C.

B. Arrival time derivatives with respect to inversion parameters

The linearization approach requires the computation of ray travel time derivatives with respect to the unknown parameters **q.** Differentiation of time with respect to source and receiver locations for the direct ray path is presented analytically in Refs. 14 and 24; bottom depth is also considered in the latter reference. The time derivatives with respect to source range r, source depth z_s, and water column depth WD are as follows.[24]

First dealing with the direct path, we recognize that

$$\frac{\partial t}{\partial WD} = 0 \tag{7}$$

because there is no interaction with the water-sediment interface. From ray theory, the derivatives for range and source depth can be shown to be

$$\frac{\partial t}{\partial r} = p, \tag{8}$$

$$\frac{\partial t}{\partial z_s} = -\frac{\sqrt{1-p^2c^2(z_s)}}{c(z_s)}, \tag{9}$$

where ray parameter p, as defined by Snell's Law, characterizes eigenrays—rays connecting source and receiver. Also $c(z)$ is the sound speed at depth z.

For the SR, we have

$$\frac{\partial t}{\partial \mathrm{WD}} = 0, \tag{10}$$

$$\frac{\partial t}{\partial r} = p, \tag{11}$$

$$\frac{\partial t}{\partial z_s} = -\frac{\sqrt{1-p^2c^2(z_s)}}{c(z_s)}. \tag{12}$$

For the bottom reflected path, the derivatives are

$$\frac{\partial t}{\partial WD} = \frac{2\sqrt{1-p^2c^2(WD)}}{c(WD)}, \tag{13}$$

$$\frac{\partial t}{\partial r} = p, \tag{14}$$

$$\frac{\partial t}{\partial z_s} = -\frac{\sqrt{1-p^2c^2(z_s)}}{c(z_s)}. \tag{15}$$

Derivatives for all paths with respect to time instant t_0 are 1.

The time derivatives require the calculation of p. For most paths, p is computed using Newton's method.[14,15,24,25] For direct, turning rays, a turning point z_m exists. In such cases, it becomes difficult to approximate the derivatives required for Newton's method, and a basic first order approximation can produce p for which $1-p^2c^2(z_m)<0$; this causes $\sqrt{1-p^2c^2(z_m)}$ to become imaginary. To handle this problem, we use the bisection method[24,26] for estimating the turning point z_m and the ray parameter p. To ensure that $\sqrt{1-p^2c^2}$ is always real, the bisection method solves for p by focusing on a small bounded region that contains the solution p and iteratively narrows the region by half until a desired tolerance is reached.

The arrival time derivatives with respect to EOF coefficients can be derived in the following way. The sound speed profile is described as

$$\mathbf{c} = \mathbf{c_m} + \sum_{i=1}^{N_e} \mu_i \mathbf{v_i}, \tag{16}$$

where $\mathbf{c_m}$ is the mean sound speed profile vector obtained from CTD measurements, $\mathbf{v_i}$, $i=1,\ldots, N_e$, are the eigenvectors of the sound speed covariance matrix, and μ_i, $i=1,\ldots, N_e$ are the eigenvector coefficients. Quantity N_e is the number of EOFs included in the system. In our case, $N_e=3$ because of prior information. Linear interpolation is used on these vectors to obtain the full profile

$$c(z) = c_m(z) + \sum_{i=1}^{N_e} \mu_i v_i(z). \tag{17}$$

Next we derive $\partial t/\partial \mu_i$ for $i=1, 2,\ldots N_e$. We can write

$$t = \int_{z_s}^{z_r} \frac{1}{c(z)\sqrt{1-p^2c^2(z)}} dz. \tag{18}$$

Note that t is dependent on both sound speed c and the ray parameter p. Differentiating t with respect to μ_i by applying the chain rule on Eq. (18) and with $\partial c/\partial \mu_i = v_i$ given by Eq. (17), we obtain

$$\begin{aligned}\frac{\partial t}{\partial \mu_i} &= \frac{\partial t}{\partial c}\frac{\partial c}{\partial \mu_i} + \frac{\partial t}{\partial p}\frac{\partial p}{\partial \mu_i} \\ &= \int_{z_s}^{z_r} \frac{\left(2p^2c^2(z)-1\right)v_i(z)}{c^2(z)\left(1-p^2c^2(z)\right)^{3/2}} dz \\ &\quad + \frac{\partial p}{\partial \mu_i}\int_{z_s}^{z_r} \frac{pc(z)}{\left(1-p^2c^2(z)^{3/2}\right)} dz.\end{aligned} \tag{19}$$

To simplify Eq. (19), we need to know $\partial p/\partial \mu_i$. We can use the following expression for range:

$$r = \int_{z_s}^{z_r} \frac{pc(z)}{\sqrt{1-p^2c^2(z)}} dz. \tag{20}$$

We also employ the fact that range does not depend on the eigenvector coefficients μ_i. It follows that

$$\begin{aligned}\frac{\partial r}{\partial \mu_i} = 0 &= \frac{\partial r}{\partial c}\frac{\partial c}{\partial \mu_i} + \frac{\partial r}{\partial p}\frac{\partial p}{\partial \mu_i} \\ &= \int_{z_s}^{z_r} \frac{pv_i(z)}{\left(1-p^2c^2(z)\right)^{3/2}} dz + \frac{\partial p}{\partial \mu_i}\int_{z_s}^{z_r} \frac{c(z)}{\left(1-p^2c^2(z)\right)^{3/2}} dz.\end{aligned} \tag{21}$$

Redistribution subject to ASA license or copyright; see http://acousticalsociety.org/content/terms. Download to IP: 128.235.24.147 On: Sun, 23 Mar 2014 17:27:53

Using Eq. (21) to cancel out the $\partial p/\partial \mu_i$ term in Eq. (19), we obtain

$$\frac{\partial t}{\partial \mu_i} = \int_{z_s}^{z_r} \frac{-v_i(z)}{c^2(z)\sqrt{1-p^2c^2(z)}} dz. \tag{22}$$

These derivatives are included in the Jacobian matrix.

C. Solving the linear system

For the linear system of Eq. (6), a simple least-squares method minimizes quantity χ^2, where

$$\chi^2 = |\mathbf{J}\delta\mathbf{q} - \delta\mathbf{t}|^2. \tag{23}$$

Quantity χ^2 is the "lack of fit" between data and arrival times generated under our model assumptions. The smaller the value, the better the fit. The solution to Eq. (23) is obtained by setting up a system of normal equations,

$$\mathbf{J}^T\mathbf{J}\delta\mathbf{q} = \mathbf{J}^T\delta\mathbf{t}, \tag{24}$$

leading to

$$\delta\mathbf{q} = (\mathbf{J}^T\mathbf{J})^{-1}\mathbf{J}^T\delta\mathbf{t}. \tag{25}$$

This approach provides the least squares solution for the parameter corrections ($\delta\mathbf{q}$). If matrix $\mathbf{J}^T\mathbf{J}$ is well-conditioned, its inverse can be reliably obtained, and $\delta\mathbf{q}$ can be easily calculated using the system of Eq. (25). However, matrix $\mathbf{J}^T\mathbf{J}$ is typically ill-conditioned.

To obtain stable and physically meaningful solutions to the inverse problem of interest, regularization can be employed making use of prior information. This method, a generalization of Tikhonov regularization, combines prior information on the unknown parameters including uncertainty and the least squares objective function.

To integrate prior information, a slight rearrangement of our system is necessary. Because the linear system of Eq. (25) is formulated in terms of parameter perturbations instead of the parameters themselves, *a priori* information for the latter cannot be incorporated directly into the system. For this information to be included, the system can be rearranged. By introducing vector $\mathbf{q_0}$ as the vector of initial conditions for the unknown parameters, manipulating Eq. (6) leads to

$$\mathbf{Jq} = \mathbf{t} = \mathbf{Jq_0} + \delta\mathbf{t}. \tag{26}$$

Solutions to the linear system of Eq. (26) are direct estimates of the parameters.

To implement regularization, a new objective function Φ, now based on Eq. (26), is minimized. The objective function is defined as[15]

$$\Phi = |\mathbf{G}(\mathbf{Jq} - \mathbf{t})|^2 + \lambda^2|\mathbf{H}(\mathbf{q} - \mathbf{q_p})|^2, \tag{27}$$

where $\mathbf{H}$ is the regularization weighting matrix, including uncertainties on those parameters for which *a priori* information is available, and $\mathbf{q_p}$ is the vector containing prior information of the components of vector $\mathbf{q}$. We also use $\mathbf{q_p}$ as the vector of initial values for the iterative regularization method. Parameter λ^2 is a Lagrange multiplier, selection of the value of which will be addressed later. Assuming that the noise for measured data (arrival times) follows a zero mean Gaussian distribution with standard deviation σ_i and assuming no correlations, $\mathbf{G}$ is a diagonal matrix defined as

$$\mathbf{G} = \mathrm{diag}[1/\sigma_1, 1/\sigma_2, \ldots, 1/\sigma_{\mathrm{KN}}]. \tag{28}$$

In our case, $\sigma_1 = \sigma_2 = \cdots = \sigma_{\mathrm{KN}}$.

The regularized solution is obtained as

$$\mathbf{q} = (\mathbf{J}^T\mathbf{G}^T\mathbf{GJ} + \lambda^2\mathbf{H}^T\mathbf{H})^{-1}(\mathbf{J}^T\mathbf{G}^T\mathbf{Gt} + \lambda^2\mathbf{H}^T\mathbf{Hq_p}). \tag{29}$$

Quantity $\lambda^2\mathbf{H}^T\mathbf{H}$ of Eq. (29) stabilizes the inversion solution, remedying the ill-conditioning. A search is conducted for an "optimal" value of λ^2 that will balance the two components of the objective function. The first is the χ^2 error (here, $\chi^2 = |\mathbf{G}(\mathbf{f}(\mathbf{q}) - \mathbf{t})|^2$), which should approach *KN* for best fit; the second expresses the deviation from prior information.

The uncertainty matrix $\mathbf{H}$ that we use is selected as

$$\mathbf{H} = \mathrm{diag}\left[1/h_{\mathrm{q1}}, 1/h_{\mathrm{q2}}, \ldots, 1/h_{\mathrm{qM}}\right], \tag{30}$$

where h_{qi} represents the uncertainty for the ith parameter of vector $\mathbf{q}$. For those parameters without *a priori* information, the corresponding term in $\mathbf{H}$ can be set to zero.

To implement regularization, we start with the initial model $\mathbf{q_p}$ and then solve Eq. (27) iteratively until convergence is achieved. Convergence is indicated when the χ^2 error approaches *KN*.

III. RESULTS FROM SYNTHETIC DATA

To carry out a performance evaluation of the new method, we conducted Monte Carlo simulations with synthetic data. Arrival times were generated for the three paths

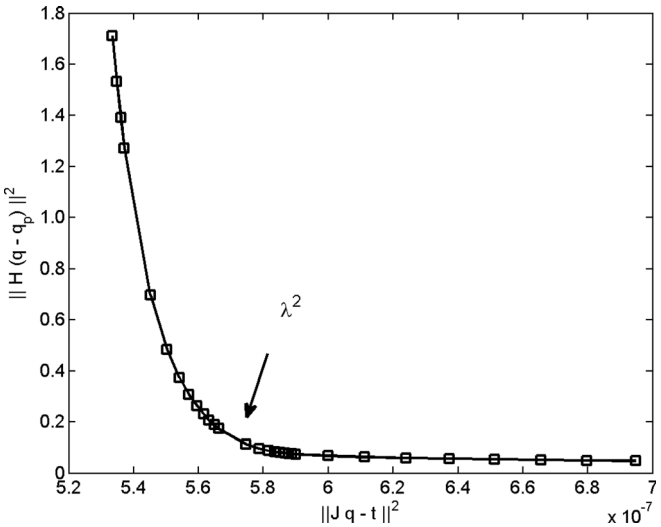

FIG. 1. The L-curve, based on which the regularization coefficient λ^2 is selected. The error in the arrival times was Gaussian-distributed with zero mean and a standard deviation of 200 ms.

Redistribution subject to ASA license or copyright; see http://acousticalsociety.org/content/terms. Download to IP: 128.235.24.147 On: Sun, 23 Mar 2014 17:27:53

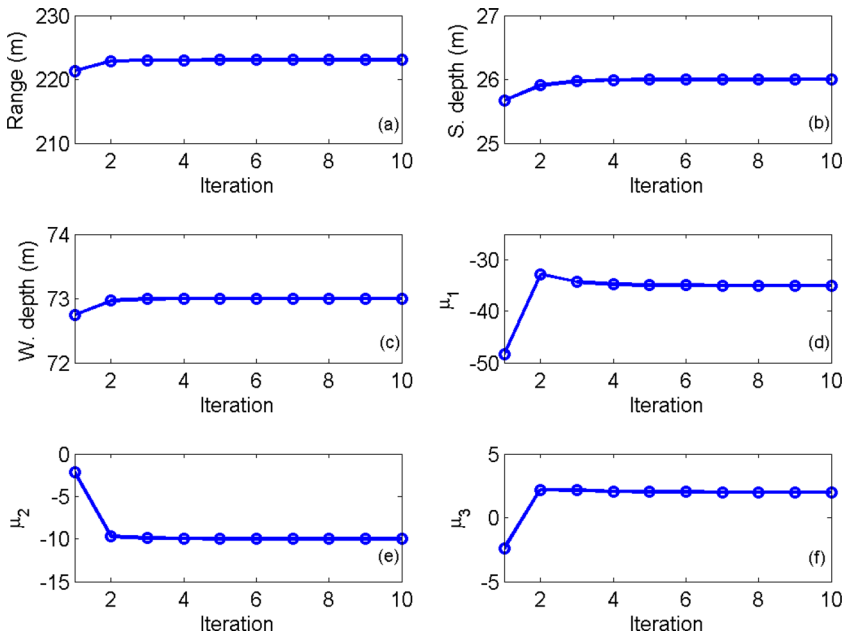

FIG. 2. (Color online) Linearization estimates vs iteration: (a) source range, (b) source depth, (c) water depth, (d) μ_1, (e) μ_2, (f) μ_3.

of interest, considering a VLA and an environment similar to that of the SW06 experiment.[22,23,27] We generated 200 noisy realizations of the arrival times for the three paths; the noise was additive, Gaussian, and zero mean with a standard deviation of 200 μs.

The coefficient λ^2 of Eq. (27) was selected by forming the L-curve (Ref. 16) of Fig. 1. We selected a value of λ^2 that helps us attain a balance between prior information (regularization term) and minimization of the simple least squares error. It has been recommended that a value of λ^2 that lies to the right of the corner of the curve is selected,[28] although there is no way to find a unique optimum value.

Figure 2 demonstrates results for a single realization vs iteration number for the linearization approach. It can be seen that only four iterations are required for convergence. PDFs from Monte Carlo runs with 200 realizations are shown in Fig. 3.

We also selected a smaller value for λ^2, which means that the least squares part of the function that is minimized is weighted more now (with the prior information impacting the solution less). Results are shown in Fig. 4. Table I presents the true values of the parameters that we estimate and the maximum a posteriori (MAP) estimates obtained from the estimation with the two values of λ^2 by maximizing the computed PDFs of Figs. 3 and 4. It is interesting to observe how the two values of λ^2 provide slightly different results for the EOF coefficients (the results for source range and depth and bottom depth are almost identical). The results from using a small value for λ^2 are very close to the true values for the coefficients. Slight discrepancies between true values and estimates are observed when a larger λ^2 is used. On the other hand, a small λ^2 results in higher uncertainty/spread in the estimation process as shown from the PDFs of Fig. 4 and their comparison to those of Fig. 3. This is the well known interplay between variability in the results

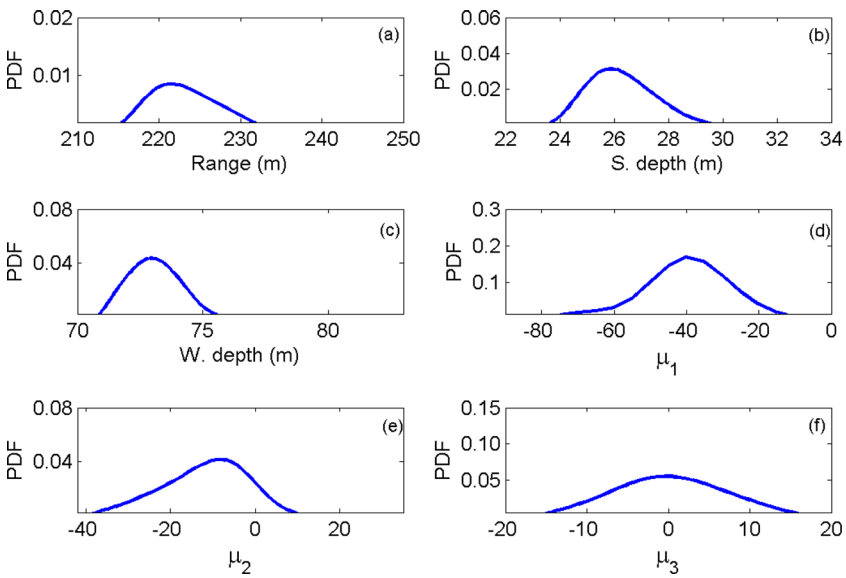

FIG. 3. (Color online) PDFs of (a) source range, (b) source depth, (c) water column depth, (d) μ_1, (e) μ_2, (f) μ_3.

Redistribution subject to ASA license or copyright; see http://acousticalsociety.org/content/terms. Download to IP: 128.235.24.147 On: Sun, 23 Mar 2014 17:27:53

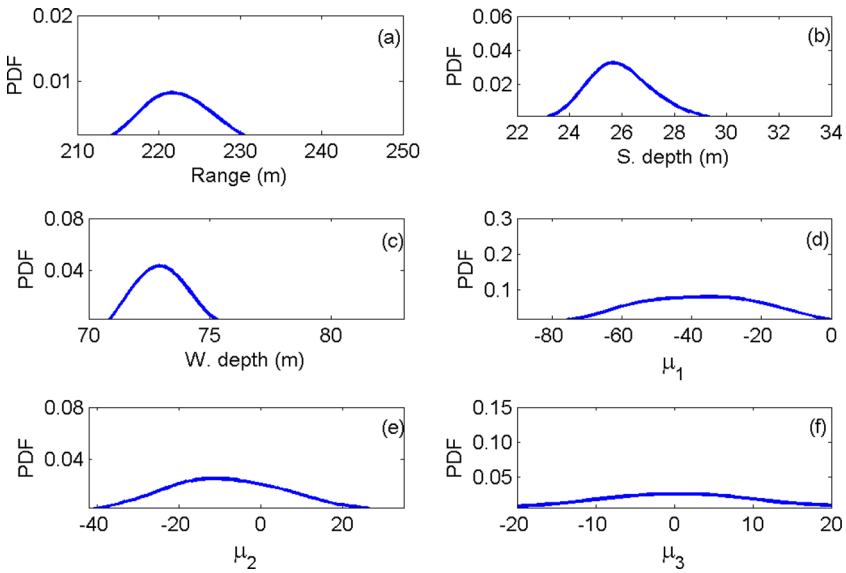

FIG. 4. (Color online) PDFs of (a) source range, (b) source depth, (c) water column depth, (d) μ_1, (e) μ_2, (f) μ_3 for a smaller value of λ^2.

(when a small amount of regularization is applied) and bias (when regularization favors the prior information). When the latter happens, the solution is biased toward the prior values, although this is evident only for μ_1 and μ_2 in our results.

We should point out here that the diagonal elements of matrix H are 1/30, 1/10, 1/40, 1/30, 1/20, 1/10, and 0 for source range, source depth, water depth, μ_1, μ_2, μ_3, and time instant, respectively, reflecting a significant amount of uncertainty regarding the available prior information: That is, the processor was not restricted within search intervals tightly surrounding the true parameter values.

Because we cannot express the quality of the complete sound speed profile through a PDF, we show in Fig. 5(a) the true sound speed profile of the water column in the synthetic environment (squares) and the MAP profile calculated from the 200 estimates we obtained (circles) for the larger value of λ^2. This estimate was calculated by using the MAP estimates for coefficients μ_1, μ_2, and μ_3. Figure 5(b) demonstrates the same two profiles, but now a few estimates obtained from distinct realizations (solid curves) are superimposed. Although these results from different realizations do not represent a full PDF, they provide an idea of the spread of the sound speed profiles around the MAP estimate and they complement Fig. 3.

To determine how "local" our method is, that is, how sensitive it is to initial conditions or prior information, we performed estimation using a different prior model (matrix **H** remained the same). The new prior assumptions are shown in Table II. Results are demonstrated in Fig. 6 and Table II and show robustness of the method: Two very different sets of prior values produced practically the same results. The PDFs are very similar to those of Fig. 3 and the MAP estimates of Table II are excellent. We should mention that the method does not always converge. For example when we use 100, 90, as 80 as prior values for the EOF coefficients, the method diverged. However, such a choice reflects a complete lack of information on the involved parameters, which is very rarely the case.

Last, to test our method in more challenging circumstances, we performed estimation employing arrival times with higher uncertainty (the standard deviation was 300 μs). The PDFs, shown in Fig. 7, demonstrate a larger spread than those of Fig. 3; this is expected because of the increased uncertainty. However, the modes of the densities are very close to the true parameter values.

TABLE I. True, prior, and estimated values for the unknown parameters for two λ^2.

Parameter	True	Prior	Estimated	Estimated small λ^2
r (m)	223	230	221.5	221.6
z_s (m)	26	30	25.9	25.7
WD (m)	73	80	73.0	72.9
μ_1	−35	−70	−40	−35
μ_2	−10	−30	−8	−11
μ_3	2	−1	0	1

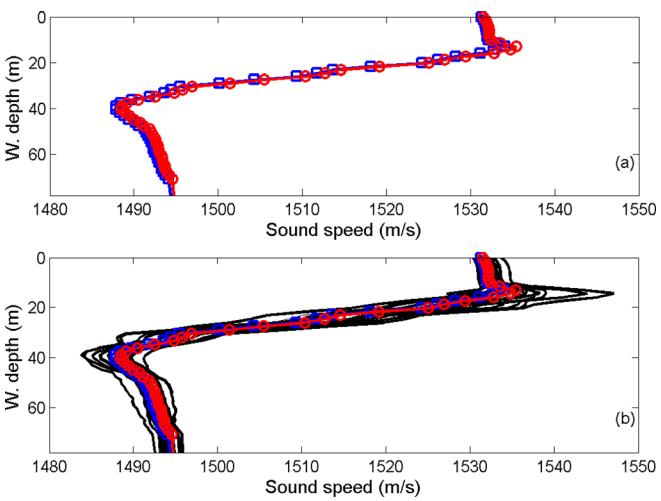

FIG. 5. (Color online) (a) The sound speed profile used for the simulations (curve with squares) and the sound speed profile constructed with the MAP estimates obtained from 200 realizations. (b) The profiles of (a) with superimposed sound speed profiles estimated from a few realizations (solid curves).

Redistribution subject to ASA license or copyright; see http://acousticalsociety.org/content/terms. Download to IP: 128.235.24.147 On: Sun, 23 Mar 2014 17:27:53

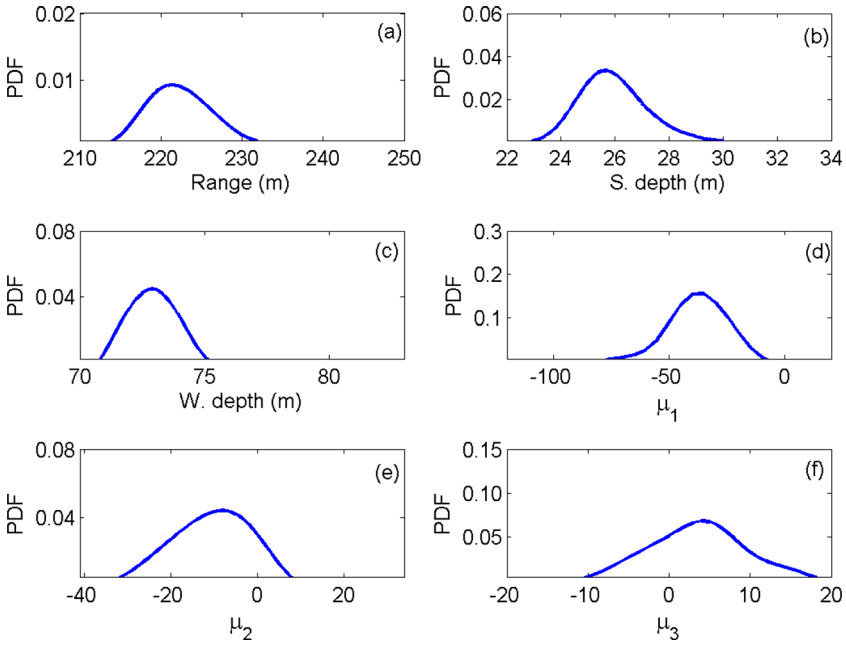

FIG. 6. (Color online) PDFs of (a) source range, (b) source depth, (c) water column depth, (d) μ_1, (e) μ_2, (f) μ_3 for a different set of prior values.

IV. PARTICLE FILTERING FOR ARRIVAL TIME ESTIMATION FROM SW06 DATA AND INVERSION RESULTS

The data we are processing in this work were collected at 16 vertically separated hydrophones that were equally spaced with a spacing of 3.75 m. The shallowest hydrophone was at roughly 20 m from the surface. The source transmitted linear frequency modulated (LFM) signals in low and mid frequencies. We investigate a case where the frequency was between 100 and 900 Hz. The time series that we are using for the inversion are the result of match-filtering the received time series with the transmitted signal. Only the 14 deepest hydrophones are used because the signal-to-noise ratio at the top two was very low. The time series are shown in Fig. 8.

The data were collected at short range (approximately 230 m) in a range-independent environment in terms of water column depth, which was reported to be around 78 m. The mean sound speed profile calculated from CTD measurements will be illustrated later in the paper.

The problem we are examining is as follows. A source is emitting a broadband pulse $s(l)$ (in our case a *sinc* after the matched-filtering process of the received signal and source pulse). Signals resulting from the propagation of the pulse through the ocean medium are received at N spatially separated hydrophones via several paths. Because of the angles of arrival of the different paths and the spatial separation of the hydrophones, the arrival time of a specific path at a receiving phone varies with phone location. The received signal at the nth phone is modeled as a sum of delayed and weighted replicas of the source signal $s(l)$, corresponding to paths that have undergone reflections (other than the direct path, which has not been reflected off any boundaries).[22,29] The sum is actually the superposition of K pulses corresponding to K multipaths. Specifically,

$$y_n(l) = \sum_{k=1}^{K} a_{\mathrm{nk}} s(l - t_{\mathrm{nk}}) + \gamma_n(l), \tag{31}$$

where $y_n(l)$ are the data at phone n and time sample l, t_{nk} is the arrival time for path k ($k = 1,\ldots, K$) at the nth receiver, and noise component $\gamma_n(l) \sim N(0, \sigma_\gamma^2)$. Weights a_{nk} are the amplitudes of the distinct arrivals, which are also unknown. We refer to Eq. (31) as the observation or measurement equation. This equation reveals that data $y_n(l)$ are related to unknown arrival times t_{nk} in a nonlinear fashion. Arrival times t_{nk} and amplitudes a_{nk} form the vector of unknown parameters, termed the state vector.

Arrival times at neighboring receivers will be in close proximity, and they evolve in space across phones in a structured manner. Particle filtering or numerical sequential Bayesian filtering is a suitable approach for exploiting such evolution in estimation and has been shown to be successful in addressing several problems in ocean acoustics.[22,30–33] Carrière *et al.* performed inversion with a similar method (ensemble Kalman filters) in Ref. 34. Working in a such a framework, we apply particle filters to the problem of arrival time estimation. We cannot apply simple Kalman filters to our case because of the nonlinearity of Eq. (31); extended and unscented Kalman filters[35–42] will not resolve the nonlinearity adequately as discussed in Ref. 43.

The approach in more detail is as follows. Focusing on arrival times for a moment, let $\mathbf{t}_n$ be the state vector,

TABLE II. True, prior, and estimated values for the unknown parameters for different prior information.

Parameter	True	Prior	Estimated
r (m)	223	180	221
z_s (m)	26	30	26
WD (m)	73	80	72
μ_1	−35	10	−35
μ_2	−10	10	−8
μ_3	2	10	4

Redistribution subject to ASA license or copyright; see http://acousticalsociety.org/content/terms. Download to IP: 128.235.24.147 On: Sun, 23 Mar 2014 17:27:53

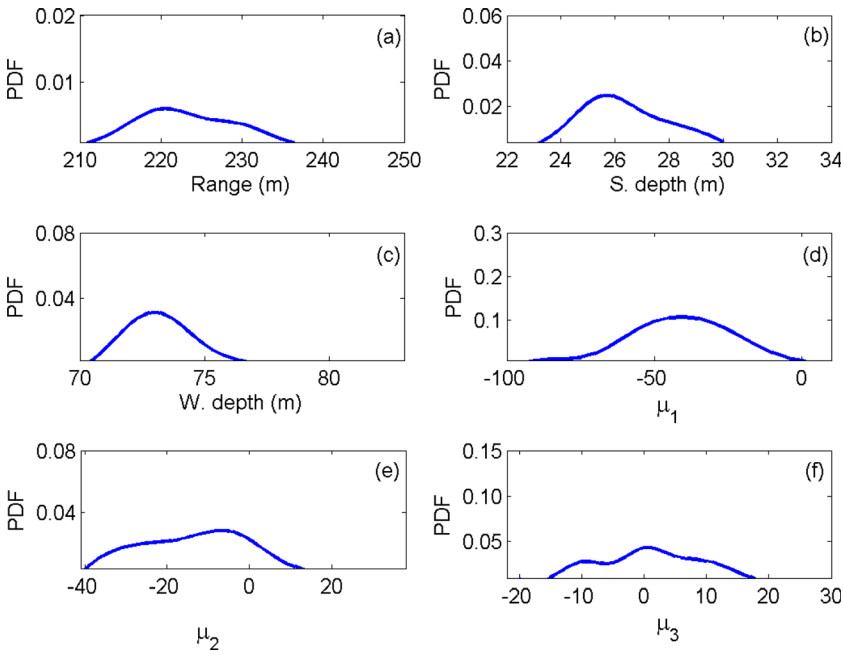

FIG. 7. (Color online) PDFs of (a) source range, (b) source depth, (c) water column depth, (d) μ_1, (e) μ_2, (f) μ_3 for an increased noise level.

consisting of these times at the nth receiver and $\mathbf{t}_n = [t_{n1},\ldots, t_{nK}]$. Let $\mathbf{y}_n$ be the received time series at receiver n and $\mathbf{Y}_n = \{\mathbf{y}_1,\ldots, \mathbf{y}_{n-1}, \mathbf{y}_n\}$. The goal is to estimate $\mathbf{t}_n$ based on the set of available measurements $\mathbf{Y}_n$. In our case, we want to estimate $p(\mathbf{t}_n|\mathbf{Y}_n)$, which will enable us to obtain point estimates for $\mathbf{t}_n$.

A particle filter consists of three steps. The first one, termed the prediction step, relies on a transition equation that predicts arrival times and amplitudes on a given hydrophone provided PDFs of those parameters estimated at the previous phone. More specifically, particles (samples) forming an arrival time PDF at state $n-1$ predict via a small perturbation arrival times at state n. The available collection of these particles constitutes a cloud. A simple transition equation for our problem reflecting this prediction is

$$\mathbf{t}_n = \mathbf{t}_{n-1} + \xi_n, \tag{32}$$

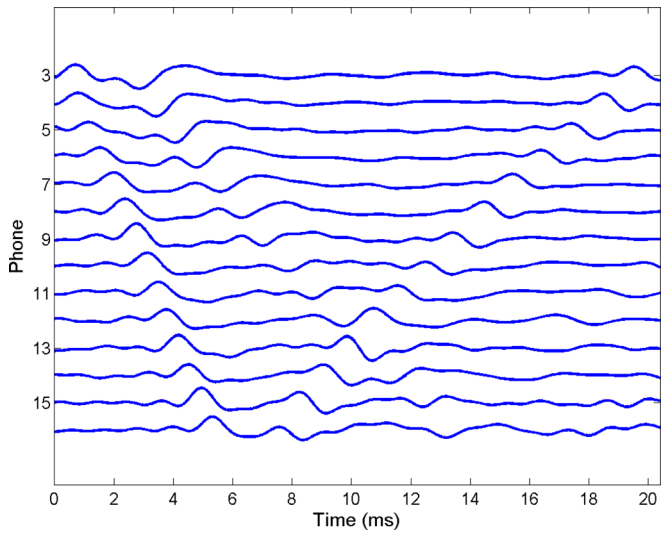

FIG. 8. (Color online) Time series at 14 hydrophones; the data were collected during the SW06 experiment.

where $\xi_n \sim N(\mathbf{0}, \Sigma)$. Σ is a $K \times K$ diagonal matrix. Diagonal elements σ_{kk} of Σ determine arrival time perturbations considered from the $(n-1)$th to the nth receiver and are selected empirically; in this work, they are the same for every state/receiver and for every arrival.

However, in Ref. 22, it was shown that including a "velocity" in the transition improves estimation performance. This gradient reflects that the spatial evolution of the arrivals varies for different paths. Using the gradient component in the transition, the effective size of the perturbation from state to state is determined individually for each path. We, therefore, have a system of two state equations,

$$\begin{aligned} \mathbf{t}_n &= \mathbf{t}_{n-1} + \dot{\mathbf{t}}_{n-1} d + \xi_n, \\ \dot{\mathbf{t}}_n &= \dot{\mathbf{t}}_{n-1} + \omega_n. \end{aligned} \tag{33}$$

Similarly to ξ_n, perturbation ω_n is distributed according to $N(\mathbf{0}, \Sigma_\omega)$. Diagonal elements σ_ω of Σ_ω represent the change in arrival time gradient from the $(n-1)$th to the nth receiver. Σ_ω is a $K \times K$ matrix as well. Parameter d was selected empirically.

The second step of a particle filter is the update process. During that stage, the particles of the unknown parameters resulting from the transition equation are updated employing the observation equation and the corresponding likelihood function

$$L(\mathbf{x}_k|\mathbf{y}_n) \propto \frac{1}{\sigma_\gamma^L s} \exp\left(-\frac{1}{2\sigma_\gamma^2} \sum_{n=1}^{L_s} \left(y_n(l) - \sum_{k=1}^{K} a_{nk} s(l - t_{nk}) \right)^2 \right), \tag{34}$$

where L_s is the length of the time series. The update stage provides a correction to the samples obtained from the prediction step; this correction stems from the new data.

Redistribution subject to ASA license or copyright; see http://acousticalsociety.org/content/terms. Download to IP: 128.235.24.147 On: Sun, 23 Mar 2014 17:27:53

Having set up the two fundamental components for sequential filtering, a particle filter was implemented utilizing the model of Eqs. (31) and (33) and was applied to SW06 time series with three prominent arrivals, D, SR, and BR. At the end of the update step, the likelihood calculations assigned a weight/probability to each particle. The particles along with their associated weights formed an estimate of the desired density $p(\mathbf{t}_n|\mathbf{Y}_n)$.

The PDF resulting from the two steps could present us with the problem of degeneracy, where only a few samples/particles obtained from the filtering process have large weights, with most particles having negligible values. A resampling step after the update can be employed to address this complication.[44] Particles are resampled with replacement from the available cloud forming the PDF of interest, using the calculated particle weights as probabilities. The particles with larger weights may be chosen a number of times and samples with small weights may not be selected at all. The new cloud of particles forms a better representation of the posterior PDF. The process consisting of a prediction, update, and resampling step is known as Sequential Importance Resampling (SIR).

The main steps of our filtering process are as follows: Arrival time samples/particles were drawn from a uniform distribution for the first phone. Using the likelihood of Eq. (34) and after the resampling step mentioned in the preceding text, a set of particles with associated weights described the PDFs of arrival times at the first phone. These arrival time particles were propagated to the second phone, were perturbed according to Eqs. (33), and were updated via the likelihood for the calculation of the PDF of arrival times at the second phone. Resampling followed. The same process was repeated until the last phone. The smoother of Ref. 45 was then implemented, which, moving from the last state backward, provides "crisper" PDFs, and, thus, estimates. The smoother employs the PDFs of arrival times at phone $n+1$ to refine the PDFs of arrival times at phone n. This process allows us to "correct" for the availability of limited information at the first phones. It should be noted that the smoother does not mandate drawing more particles after the completion of the forward filter. The smoothing process just calibrates the probabilities corresponding to already drawn particles. The number of particles for the SIR filter was 5000. Only 500 particles were used in the backward filter implementation.

As mentioned before, the amplitudes of the different arrivals were also unknown. To ensure an efficient process, amplitudes did not enter the vector of unknown parameters with particles drawn and perturbed at every state but were instead computed using a MAP estimator. Because the conditional PDFs of amplitudes on arrival times follow a Gaussian density, estimation is straightforward. We used the approach found in Refs. 29, 46, and 47 to obtain amplitude MAP estimates conditional on the arrival time particles. Specifically, for an arrival time particle $\mathbf{t}^i=[t_1^i,\ldots,t_K^i]$ at the nth phone, the MAP estimate of $\mathbf{A}^i_{\mathrm{MAP},n,}$, a vector consisting of the amplitude estimates for that arrival time particle vector at state/phone n, can be calculated as[46]

$$\mathbf{A}^i_{MAP,n}=\Theta_n^{-1}\phi_n, \tag{35}$$

where $\phi_n=\sum_{l=1}^{L_s} s(l-t^i_{\mathrm{nk}})\mathbf{y}_n(l), k=1,\ldots, K;$ $\mathbf{y}_n(l)$ is the received time series and $s(l)$ is the transmitted pulse. Also,

$$\Theta_n=\begin{pmatrix}\theta_{n11} & \theta_{n12} & \cdots & \theta_{n1K}\\ \theta_{n21} & \theta_{n22} & \cdots & \theta_{n2K}\\ \cdots & \cdots & \cdots & \cdots\\ \theta_{\mathrm{nK1}} & \theta_{\mathrm{nK2}} & \cdots & \theta_{\mathrm{nKK}}\end{pmatrix}, \tag{36}$$

where $\theta_{ni_kj_k}=\sum_{l=1}^{L_s} s(l-t^i_{ni_k})s(l-t^i_{nj_k}), i_k,j_k=1,\ldots,K.$

Using SIR, MAP amplitude estimation, and smoothing as just described, we obtained the PDFs for three path arrivals, which are shown in Fig. 9. The PDFs were constructed from the 500 sampled particles and their associated probabilities. These arrival time particles are used as input to the linearized system of Eq. (26) (data $\mathbf{t}$). For every set of three arrival times within a particle, a solution is obtained for the unknown parameters (vector $\mathbf{q}$) using Eq. (29). These multiple solutions/estimates form PDFs for the unknown parameters. PDFs for source range and depth, water column depth, and EOF coefficients μ_1, μ_2, μ_3 are shown in Fig. 10. Array tilt was also set as an unknown quantity. MAP parameter estimates along with the considered prior information are listed in Table III. The diagonal elements of the uncertainty matrix H were 1/3, 1/2, 1/3, 1/30, 1/20, 1/10, and 1/2 for range, source depth, water column depth, μ_1, μ_2, μ_3, and tilt, respectively.

Range and source depth and water column depth estimates are very close to the true values provided to us with the data. The estimates we obtained for μ_1 and μ_2 are very similar to the ones obtained for the same coefficients in Refs. 22 and 23. The estimate for μ_3 somewhat differs from those in Ref. 23 but agrees with estimates reported in Ref. 22 (the values within those references vary among themselves as well). It should be noted that the data collection sites differ for the different inversions.

In Fig. 11, we demonstrate the fit between the true time series (solid lines) and the synthetic time series, generated using the estimates shown in Table III (dotted lines). The

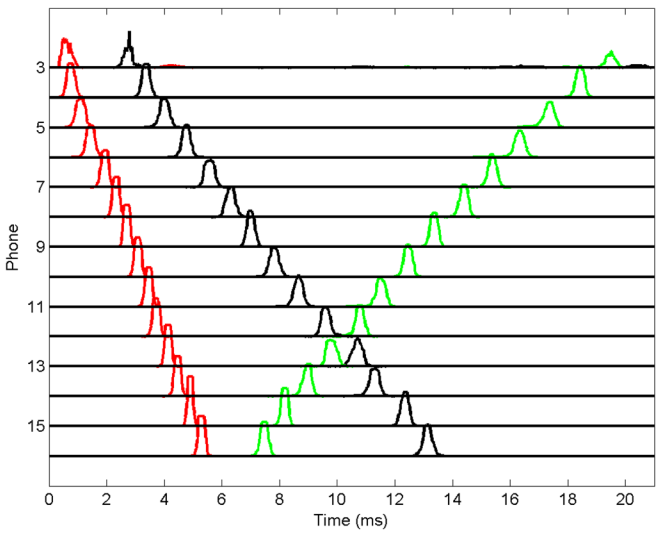

FIG. 9. (Color online) Posterior PDFs for multipath arrival times for the time series of Fig. 8.

Redistribution subject to ASA license or copyright; see http://acousticalsociety.org/content/terms. Download to IP: 128.235.24.147 On: Sun, 23 Mar 2014 17:27:53

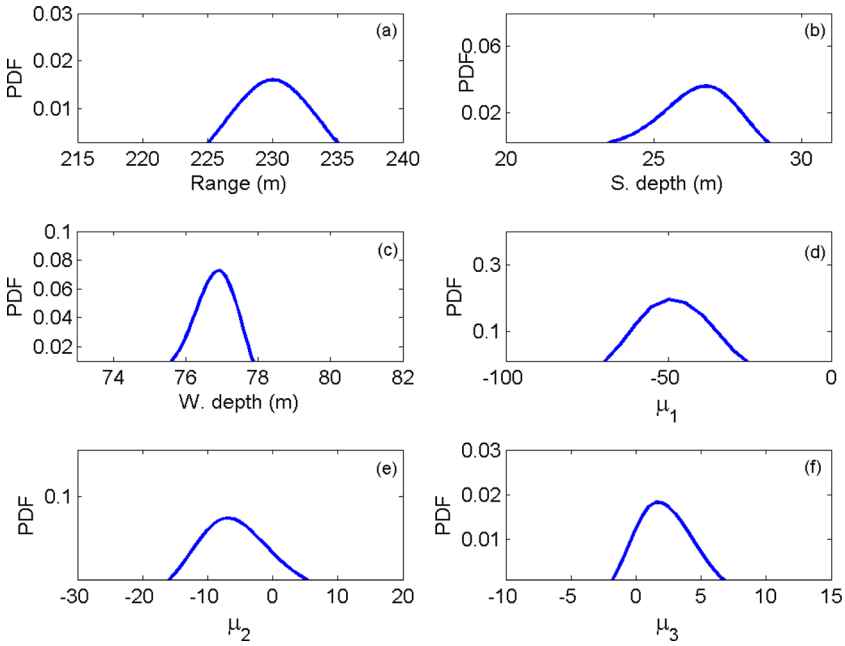

FIG. 10. (Color online) PDFs of (a) source range, (b) source depth, (c) water column depth, (d) μ_1, (e) μ_2, (f) μ_3 for real data.

arrival times $\mathbf{t}_{MAP}$ of the synthetic time series were created using ray tracing for the MAP parameter estimates of the table. The fit appears to be very good, indicating that the inversion was successful. A perfect match was not expected because the linearization process provides an approximation.

The inversion was repeated with alternative prior information to the one presented in Table III. Results from all inversions were very close.

Figure 12(a) shows the mean sound speed profile of the water column calculated from CTD measurements (squares) and the MAP profile calculated from arrival time estimates and linearization (circles). Figure 12(b) demonstrates the same two profiles, but now sound speed profiles from distinct arrival time particles (solid curves) are superimposed.

To further validate the potential and accuracy of our linearization method, we compared our results to estimates obtained from a global optimization technique for the same arrival time particles that were used for our inversion. For global optimization, we used fast simulated annealing. The process searched for the set of unknown parameters that minimize the mean squared error between the true arrival times (that is, the arrivals extracted from the SW06 time series with the PF) and replica arrival times calculated with ray tracing for that set of parameters, similarly to Ref. 11. The search intervals were the same as those employed in Ref. 22. Table IV presents inversion results for two sets of arrival time estimates using linearization and simulated annealing. There is a very good agreement between the results for both cases, indicating that both methods are successful (being consistent among themselves and with values reported in our references). This was expected for the global optimization-matching process because it relies on calculating the arrival times of a replica signal for multiple sets of unknown parameter values, optimizing the search for identifying the best set; no approximation to the forward model is performed. It appears that the linearization process, although it is based on an approximation and uses only a few calculations, performs equally well. Specifically, in terms of efficiency, the linearization method required six iterations (typically four to converge, but we continued to six), whereas the annealing process in our case involved seven ray tracing runs, one for each unknown parameter, for 1200

TABLE III. Prior information and MAP parameter estimates for source range and depth, water column depth, EOF coefficients μ_1, μ_2, μ_3, and tilt.

Parameter	Prior	MAP Estimate
r (m)	230	230
z_s (m)	25	26.8
WD (m)	79	76.9
μ_1	−85	−50
μ_2	−55	−7
μ_3	2	1.5
Tilt (°)	0	−0.2

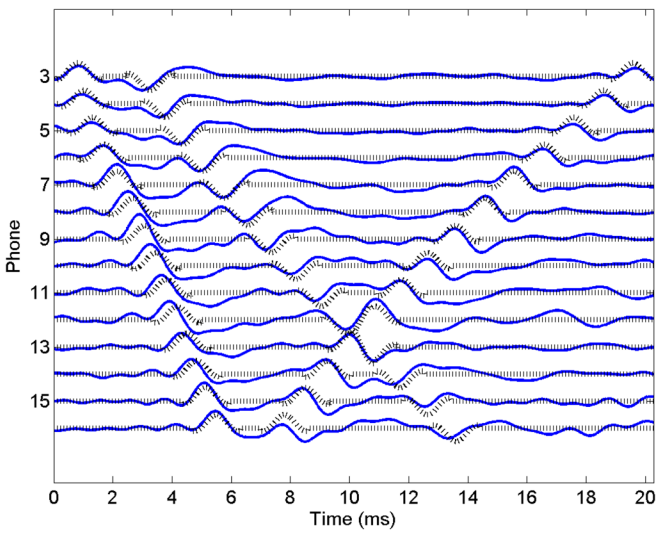

FIG. 11. (Color online) Real data (solid lines) and synthetic time series (dotted lines) generated using the linearization estimates.

Redistribution subject to ASA license or copyright; see http://acousticalsociety.org/content/terms. Download to IP: 128.235.24.147 On: Sun, 23 Mar 2014 17:27:53

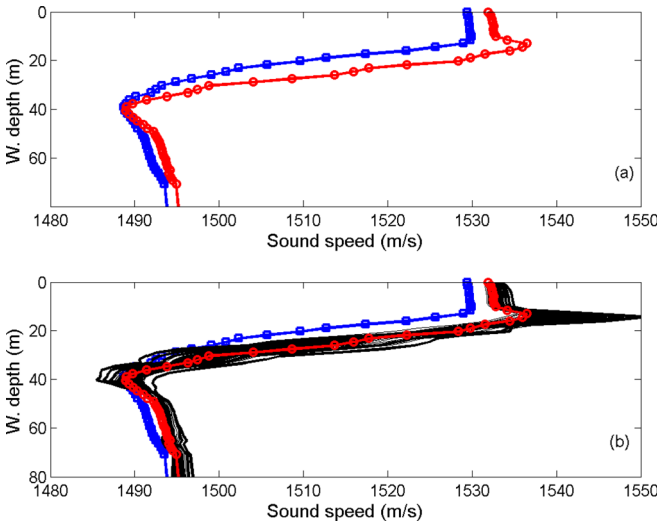

FIG. 12. (Color online) (a) The mean sound speed profile as calculated by CTD measurements (squares) and the sound speed profile constructed with the MAP estimates obtained from the extracted arrival time PDFs (circles). (b) The profiles of (a) with superimposed sound speed profiles constructed from distinct arrival time particles (solid curves).

iterations. This significant difference demonstrates the efficiency of our method, which does not come at the expense of accuracy.

V. CONCLUSIONS

A new approach is proposed for the estimation of source location parameters and array tilt, water depth, and water column sound speed profile using multipath arrival times and linearization. The process makes use of a Jacobian matrix that includes arrival time derivatives with respect to EOF coefficients in addition to those with respect to source location, tilt, and water depth, which have been used in previous work. Simulations validated the new approach for two noise levels and different prior information. Comparing results we concluded that the method was robust with respect to both noise and initial conditions/prior assumptions. We also observed that the value of a Largrange multiplier necessary for the implementation of the method played a role in the estimation results: This value can reduce uncertainty significantly (a substantial advantage of the method) but may introduce a small bias.

The method was tested on real data with arrival times extracted from SW06 time series using particle filtering.

TABLE IV. Parameter estimates using the linearization method for two sets of arrival times resulting from the PF and corresponding simulated annealing (SA) results for the same arrival times.

Parameter	Linear Estimate	SA Estimate	Linear Estimate	SA Estimate
r (m)	228	231	232	231
z_s (m)	26	26	27	27
WD (m)	76	76	77	77
μ_1	−54	−56	−42	−43
μ_2	−10	−12	−7	−7
μ_3	2	1	2	−2
Tilt (°)	0	0	0	0

PDFs of arrivals at a number of phones were smoothed (filtered) to obtain the smallest variance estimates by relating arrival times at neighboring phones.

These arrival time particles were then used as input for the inverse problem. The solutions formed PDFs for the unknown parameters from which MAP estimates were calculated. Comparison was made to ground-truth information, estimates reported by other authors, and estimates from fast simulated annealing. All results are similar. The new algorithm has significant advantages of efficiency: Convergence required only a few iterations per inversion, whereas simulated annealing involved many more; accurate estimates are obtained without the need for extensive prior information or onerous computations.

ACKNOWLEDGMENTS

This work was supported by the Office of Naval Research through Grants N000141010073 and N000141310077.

[1]A. Tolstoy, *Matched Field Processing for Underwater Acoustics* (World Scientific, Singapore, 1993), pp. 1–212.
[2]E. Livingston and O. Diachok, "Estimation of average under-ice reflection amplitudes and phases using matched-field processing," J. Acoust. Soc. Am. **86**, 1909–1919 (1989).
[3]A. Tolstoy, "Linearization of the matched field processing approach to acoustic tomography," J. Acoust. Soc. Am. **91**, 781–787 (1992).
[4]M. D. Collins, W. A. Kuperman, and H. Schmidt, "Nonlinear inversion for ocean-bottom properties," J. Acoust. Soc. Am. **92**, 2770–2783 (1992).
[5]P. Gerstoft, "Inversion of seismoacoustic data using genetic algorithms and a posteriori probability distributions," J. Acoust. Soc. Am. **95**, 770–782 (1994).
[6]J. Shorey, L. Nolte, and J. Krolik, "Computationally efficient Monte Carlo estimation algorithms for matched field processing in uncertain ocean environments," J. Comput. Acoust. **2**, 285–314 (1994).
[7]S. E. Dosso, "Quantifying uncertainty in geoacoustic inversion. I. A fast Gibbs sampler approach," J. Acoust. Soc. Am. **111**, 129–142 (2002).
[8]D. P. Knobles, R. A. Koch, L. A. Thompson, K. C. Focke, and P. E. Eisman, "Broadband sound propagation in shallow water and geoacoustic inversion," J. Acoust. Soc. Am. **113**, 205–222 (2003).
[9]M. D. Collins and W. Kuperman, "Focalization: Environmental focusing and source localization," J. Acoust. Soc. Am. **90**, 1410–1422 (1991).
[10]Z.-H. Michalopoulou and U. Ghosh-Dastidar, "Tabu for matched-field source localization and geoacoustic inversion," J. Acoust. Soc. Am. **115**, 135–145 (2004).
[11]E. K. Westwood and D. P. Knobles, "Source track localization via multipath correlation matching," J. Acoust. Soc. Am. **102**, 2645–2654 (1997).
[12]L. Jaschke, "Geophysical inversion by the freeze bath method with an application to geoacoustic ocean bottom parameter estimation," Master's thesis, University of Victoria, Victoria, BC, Canada, 1997.
[13]S. M. Jesus, M. B. Porter, Y. Stephan, X. Demoulin, O. C. Rodriguez, and E. M. M. F. Coelho, "Single hydrophone source localization," IEEE J. Ocean. Eng. **25**, 337–346 (2000).
[14]S. E. Dosso, M. R. Fallat, B. J. Sotirin, and J. L. Newton, "Array element localization for horizontal arrays via Occam's inversion," J. Acoust. Soc. Am. **104**(2), 846–859 (1998).
[15]S. E. Dosso, G. H. Brooke, S. J. Kilistoff, B. J. Sotirin, V. K. McDonald, M. R. Fallat, and N. E. Collison, "High-precision array element localization for vertical line arrays in the Arctic Ocean," IEEE J. Ocean. Eng. **23**, 365–379 (1998).
[16]Z.-H. Michalopoulou and X. Ma, "Source localization in the Haro Strait Primer experiment using arrival time estimation and linearization," J. Acoust. Soc. Am. **118**, 2924–2933 (2005).
[17]A. Tolstoy, "Simulated performance of acoustic tomography via matched field processing," J. Comput. Acoust. **2**, 1–10 (1994).
[18]A. Tarantola, *Inverse Problem Theory* (SIAM, Philadelphia, PA, 2004), pp. 1–332.

Redistribution subject to ASA license or copyright; see http://acousticalsociety.org/content/terms. Download to IP: 128.235.24.147 On: Sun, 23 Mar 2014 17:27:53

[19]W. Menke, *Geophysical Data Analysis: Discrete Inverse Theory* (Academic, San Diego, 1984), pp. 7–280.
[20]R. E. Davis, "Predictability of sea surface temperature and sea level pressure anomalies over the North Pacific Ocean," J. Phys. Ocean. **6**, 249–266 (1976).
[21]Z.-H. Michalopoulou and R. Jain, "Particle filtering for arrival time tracking in space and source localization," J. Acoust. Soc. Am. **132**, 3041–3052 (2012).
[22]C.-F. Huang, P. Gerstoft, and W. S. Hodgkiss, "Effect of ocean sound speed uncertainty on matched-field geoacoustic inversion," J. Acoust. Soc. Am. **123**, EL162–EL168 (2008).
[23]C. Yardim, P. Gerstoft, and W. S. Hodgkiss, "Sequential geoacoustic inversion at the continental shelfbreak," J. Acoust. Soc. Am. **131**, 1722–1732 (2012).
[24]X. Ma, "Efficient inversion methods in underwater acoustics," Ph.D. thesis, New Jersey Institute of Technology, Newark, NJ (2001).
[25]S. E. Dosso and B. Sotirin, "Optimal array element localization," J. Acoust. Soc. Am. **106**, 3445–3459 (1999).
[26]J. D. Faires and R. L. Burden, *Numerical Methods* (Cengage Learning, Boston, MA, 2012), pp. 1–518.
[27]Y.-M. Jiang, N. R. Chapman, and P. Gerstoft, "Short range travel time geoacoustic inversion with vertical line array," J. Acoust. Soc. Am. **124**, EL135–EL140 (2008).
[28]P. C. Hansen, *Rank-Deficient and Discrete Ill-Posed Problems: Numerical Aspects of Linear Inversion* (SIAM, Philadelphia, PA, 1998), pp. 1–214.
[29]Z.-H. Michalopoulou and M. Picarelli, "Gibbs sampling for time-delay and amplitude estimation in underwater acoustics," J. Acoust. Soc. Am. **117**, 799–808 (2005).
[30]I. Zorych and Z.-H. Michalopoulou, "Particle filtering for dispersion curve tracking in ocean acoustics," J. Acoust. Soc. Am. **124**, EL45–EL50 (2008).
[31]C. Yardim, P. Gerstoft, and W. S. Hodgkiss, "Tracking of geoacoustic parameters using Kalman and particle filters," J. Acoust. Soc. Am. **125**, 746–760 (2009).
[32]C. Yardim, P. Gerstoft, and W. S. Hodgkiss, "Geoacoustic and source tracking using particle filtering: Experimental results," J. Acoust. Soc. Am. **128**, 75–87 (2010).
[33]J. Dettmer, S. E. Dosso, and C. W. Holland, "Sequential trans-dimensional Monte Carlo for range-dependent geoacoustic inversion," J. Acoust. Soc. Am. **129**, 1794–1806 (2011).
[34]O. Carrière, J.-P. Hermand, and J. V. Candy, "Inversion for time-evolving sound-speed field in a shallow ocean by Ensemble Kalman Filtering," IEEE J. Ocean. Eng. **34**, 586–602 (2009).
[35]J. V. Candy and E. J. Sullivan, "Ocean acoustic signal processing: A model-based approach," J. Acoust. Soc. Am. **92**, 3185–3201 (1992).
[36]J. Candy and E. Sullivan, "Sound velocity profile estimation: A system theoretic approach," IEEE J. Ocean. Eng. **18**, 240–252 (1993).
[37]J. V. Candy and E. J. Sullivan, "Model-based processor design for a shallow water ocean acoustic experiment," J. Acoust. Soc. Am. **95**, 2038–2051 (1994).
[38]J. V. Candy and E. J. Sullivan, "Passive localization in ocean acoustics: A model-based approach," J. Acoust. Soc. Am. **98**, 1455–1471 (1995).
[39]J. V. Candy and E. J. Sullivan, "Broadband model-based processing for shallow ocean environments," J. Acoust. Soc. Am. **104**, 275–287 (1998).
[40]J. V. Candy and D. H. Chambers, "Model-based dispersive wave processing: A recursive Bayesian solution," J. Acoust. Soc. Am. **105**, 3364–3374 (1999).
[41]E. J. Sullivan, J. D. Holmes, W. M. Carey, and J. F. Lynch, "Broadband passive synthetic aperture: Experimental results," J. Acoust. Soc. Am. **120**, EL49–EL54 (2006).
[42]S. Julier, J. Uhlmann, and H. F. Durrant-White, "A new method for nonlinear transformation of means and covariances in filters and estimators," IEEE Trans. Automat. Control **45**, 477–482 (2000).
[43]R. Jain and Z.-H. Michalopoulou, "A particle filtering approach for multipath arrival time estimation from acoustic time series," J. Acoust. Soc. Am. **126**, 2249–2249 (2009).
[44]B. Ristic, N. Gordon, and S. Arulampalam, *Beyond the Kalman Filter: Particle Filters for Tracking Applications* (Artech House, Boston, MA, 2004), pp. 3–292.
[45]S. J. Godsill, A. Doucet, and M. West, "Monte Carlo smoothing for nonlinear time series," J. Am. Stat. Assoc. **99**, 156–168 (2004).
[46]J. E. Ehrenberg, T. E. Ewart, and R. D. Morris, "Signal processing techniques for resolving individual pulses in a multipath signal," J. Acoust. Soc. Am. **63**, 1861–1865 (1978).
[47]C. Andrieu and A. Doucet, "Joint Bayesian model selection and estimation of noisy sinusoids via reversible jump MCMC," IEEE Trans. Signal Process. **47**, 2667–2676 (1999).

Redistribution subject to ASA license or copyright; see http://acousticalsociety.org/content/terms. Download to IP: 128.235.24.147 On: Sun, 23 Mar 2014 17:27:53